Acta Cryst. (1983). A**39**, 531–533

Determination of the Space Group of $LiZnTa_3O_9$ by Convergent-Beam Electron Diffraction

BY C. Y. YANG, Y. Q. ZHOU AND K. K. FUNG

Institute of Physics, Academia Sinica, Beijing, China

(*Received* 16 *August* 1982; *accepted* 26 *January* 1983)

Abstract

$LiZnTa_3O_9$ crystal is rhombohedral, $a_h = 5{\cdot}24$ (1) and $c_h = 14{\cdot}03$ (1) Å in the hexagonal system, $Z = 2$, $D_m = 7{\cdot}61$ g cm^{-3}. Its space group, determined by convergent-beam electron diffraction, is $R\bar{3}c$.

Technologically important ferroelectric $LiNbO_3$ and $LiTaO_3$ crystals have been the subject of intensive study (Abrahams, Reddy & Bernstein, 1966; Abrahams & Bernstein, 1967). Study of compounds related to the lithium niobate and lithium tantalate family has been hampered by the difficulty of obtaining good quality single crystals. Polycrystalline $LiZnTa_3O_9$, which is related to $LiTaO_3$, has been prepared by Kutolin, Revzina & Naschina (1967). Recently, single crystals of $LiZnTa_3O_9$ have been grown in our institute (Shu, Xia, Chen, Jiang, Zhang & Yu, 1981). A convergent-beam electron-diffraction (CBED) study has been undertaken to determine its space group. It is well known that CBED is a very useful technique for the determination of point groups and space groups (Goodman, 1975; Buxton, Eades, Steeds & Rackham, 1976). In CBED, higher-order Laue-zone (HOLZ) effects, which are usually neglected in the projection approximation or zero-order Laue zone, become very important. HOLZ diffraction provides three-dimensional information which facilitates the determination of lattice parameters and crystal symmetry.

Specimens of $LiZnTa_3O_9$ were obtained by grinding a bulk crystal into small crystallites ranging from 0·5 to 5 μm. The crystallites were supported on carbon film on copper grids for observation in a Philips EM 400 electron microscope. The microscope, fitted with a STEM pole piece, was operated in the TEM mode and a probe size of about 40 nm was used.

Convergent-beam zone-axis patterns (ZAPs) obtained can be readily indexed in the trigonal or rhombohedral system. Figs. 1 and 2 show the $3m$ symmetry. This is the [0001] ZAP. It is the highest symmetry pattern. Other ZAPs are of lower symmetry, for instance, the symmetry of the $[1\bar{1}01]$ ZAP is m (Fig. 3*a*). It should be pointed out that the symmetry of the patterns is not perfect. A close examination of Fig. 1 shows that there is some variation in the intensity and the shape of the HOLZ lines in the bright-field disc. Fig. 3(*a*) also shows signs of asymmetry along the mirror plane. There are clear differences between the upper pair reflections and the bright-field mirror is also not perfect. These CBED patterns were obtained from small crystallites ground from the bulk. Such crystallites are not parallel-sided slabs and they are seldom defect free. CBED from such crystallites will inevitably show signs of slight asymmetry. Therefore, care must be exercised in determining the symmetry of the patterns. CBED patterns from different zone axes should be considered for self-consistency. The lattice parameters of $LiZnTa_3O_9$, obtained from combined CBED and conventional electron diffraction, are $a_h = 5{\cdot}24$ (1), $c_h = 14{\cdot}03$ (1) Å, where h refers to the hexagonal system. In the rhombohedral system, the lattice parameters are $a = 5{\cdot}57$ (1) Å and $\alpha = 56{\cdot}12$ (17)°.

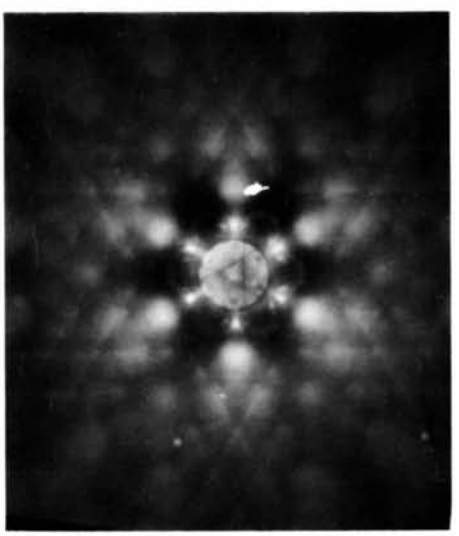

Fig. 1. [0001] ZAP of $LiZnTa_3O_9$ at 120 kV. Both the central bright-field disc and the whole-pattern symmetry are $3m$. However, the symmetry is not perfect. The HOLZ lines in the bright-field disc show signs of variation in intensity and sharpness.

0108-7673/83/040531-03$01.50

The bright-field and whole-pattern symmetry of the [0001] ZAP (Figs. 1 and 2) are both $3m$. According to Buxton *et al.* (1976), this implies that the diffraction group can be either $3m$ or ${}_6{}_R m m_R$ corresponding to point group $3m$ or $\bar{3}m$, which can be distinguished by their dark-field symmetry. Consider the $[1\bar{1}01]$ zone axis, the diffraction groups for $3m$ and $\bar{3}m$ are m and ${}_2{}_R m m_R$, respectively. Fig. 3 shows that the bright-field and whole-pattern symmetries are both m, and the $\pm(11\bar{2}0)$ dark-field symmetries are also m, the dark-field mirror being parallel to that of the bright field. Here we have neglected the slight asymmetry of the patterns arising from imperfect crystals. In fact, the dark-field mirror is derived from the symmetry element m_R. The $\pm(11\bar{2}0)$ dark fields are related by ${}_2{}_R$. Therefore, the crystal has an inversion centre so the point group must be $\bar{3}m$. The same result can also be obtained from the $\pm(11\bar{2}0)$ dark field of the [0001] ZAP.

Furthermore, systematic-extinction rules obtained by indexing diffraction patterns are $-h + k + l = 3n$ for general reflections, and $l = 2n$, $h + k = 3n$ for $h\bar{h}0l$ reflections. These rules are consistent with space group $R\bar{3}c$. The presence of the glide plane is confirmed by the extinction line in the $(8\bar{8}01)$ disc along the mirror plane in Fig. 4 (Gjønnes & Moodie, 1965; Steeds, Rackham & Shannon, 1978). Fig. 4 is obtained by rotating the specimen about a $\langle 11\bar{2}0\rangle$ axis from the [0001] orientation. The extinction line is due to a glide plane in the c direction. The space group of $LiZnTa_3O_9$ is therefore $R\bar{3}c$.

It is interesting to note that the space group of ferroelectric $LiTaO_3$ is $R3c$ and that of paraelectric $LiTaO_3$ is $R\bar{3}c$. The Curie temperature of $LiTaO_3$ is

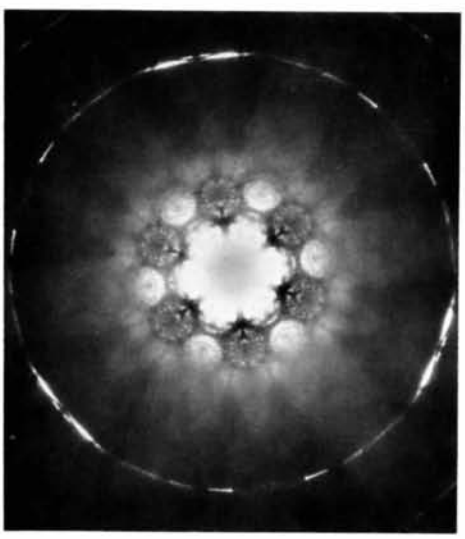

Fig. 2. [0001] ZAP of $LiZnTa_3O_9$ showing HOLZ rings. Note that the symmetry of the first-order Laue-zone ring is $3m$.

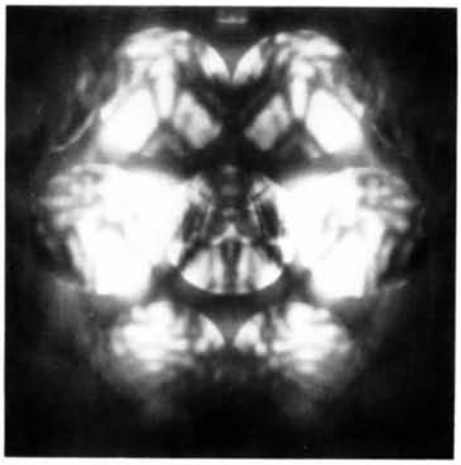

(*a*)

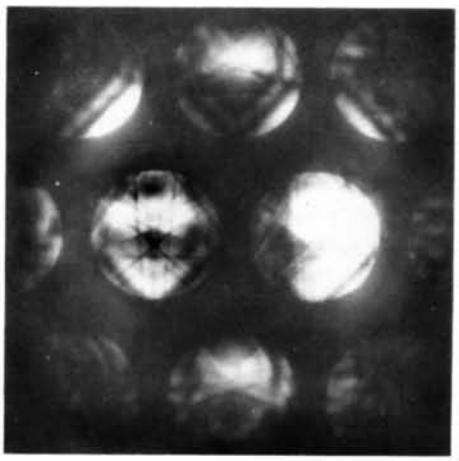

(*b*)

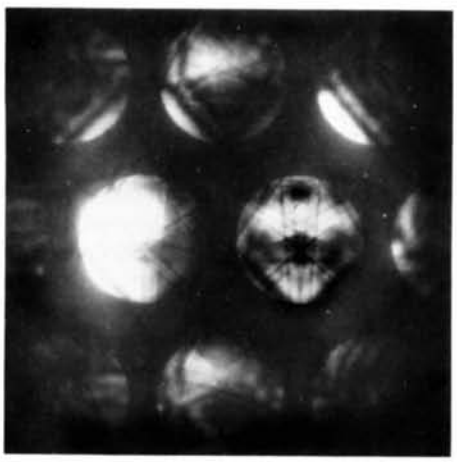

(*c*)

Fig. 3. $[1\bar{1}01]$ ZAP of $LiZnTa_3O_9$. (*a*) On axis ZAP showing the m symmetry of the bright-field and the whole patterns. (*b*) and (*c*) $\pm(11\bar{2}0)$ dark-field patterns. The internal symmetry is m. The conjugate $\pm(11\bar{2}0)$ dark-field are related by ${}_2{}_R$. We note that there are signs of slight asymmetry in the ZAPs arising from imperfections in the specimen.

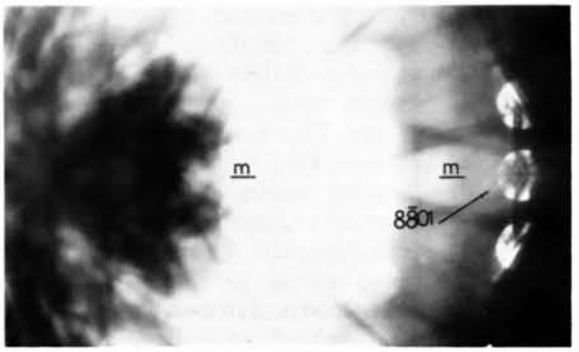

Fig. 4. Excitation of the 8$\bar{8}$01 reflection, showing an extinction line along the mirror plane of the whole pattern. The extinction in this case is due to a *c* glide.

938 K. By analogy with $LiTaO_3$, we conclude that $LiZnTa_3O_9$ at room temperature is paraelectric and that the addition of Zn to $LiTaO_3$ lowers its Curie temperature. The density of $LiTaO_3$, D_m is 7·4564 g cm^{-3}. There are six molecular units per hexagonal unit cell. For $LiZnTa_3O_9$, $D_m = 7{\cdot}61$ g cm^{-3} and $Z = 2$ per hexagonal unit cell (Shu *et al.*, 1981).

We are grateful to Mr Q. M. Shu for providing us with single crystals of $LiZnTa_3O_9$.

References

ABRAHAMS, S. C. & BERNSTEIN, J. L. (1967). *J. Phys. Chem. Solids*, **28**, 1685–1692.
ABRAHAMS, S. C., REDDY, J. M. & BERNSTEIN, J. L. (1966). *J. Phys. Chem. Solids*, **27**, 997–1012.
BUXTON, B. F., EADES, J. A., STEEDS, J. W. & RACKHAM, G. M. (1976). *Philos. Trans. R. Soc. London Ser. A*, **281**, 171–194.
GJØNNES, J. & MOODIE, A. F. (1965). *Acta Cryst.* **19**, 65–67.
GOODMAN, P. (1975). *Acta Cryst.* A**31**, 804–810.
KUTOLIN, S. A., REVZINA, T. V. & NASCHINA, N. I. (1967). *Dokl. Akad. Nauk SSSR*, **175**, 407–410 (in Russian).
SHU, Q. M., XIA, H. C., CHEN, Y. P., JIANG, Y. D., ZHANG, Y. Z. & YU, L. (1981). Abstracts of the 1981 Annual Meeting of the Chinese Silicate Society, Beijing, pp. 118–119 (in Chinese).
STEEDS, J. W., RACKHAM, G. M. & SHANNON, M. D. (1978). *Electron Diffraction* 1927–1977, Institute of Physics Conference Series No. 41, pp. 135–139.

Acta Cryst. (1983). A**39**, 533–538

X-ray Debye–Waller Factors of Zinc-Blende-Structure Materials:– Dynamic Deformation Effects

BY JOHN S. REID

Department of Natural Philosophy, The University, Aberdeen AB9 2UE, Scotland

(*Received* 5 *October* 1982; *accepted* 26 *January* 1983)

Abstract

A discussion is given on simple grounds, not explicitly involving the dynamical deformation formalism, of the implications of having the outer part of the electron distribution vibrating significantly differently from the core. The use of a lattice dynamical shell model to represent this effect is examined in some detail, with particular reference to the framework within which such a model gives meaningful results. Predictions are given from the 14-parameter shell models and the 11-parameter valence-shell models for the difference between Debye–Waller B values of the shells and cores and also for the effective Debye–Waller factors for the deforming ions in 14 zinc-blende-structure compounds. It is concluded that the effective X-ray Debye–Waller B at very small $\sin\theta/\lambda$ is typically several percent smaller than the core B value, owing to a very substantial reduction in the mean-square displacements of shells compared with cores. Results are also given for the 15-parameter deformation-dipole models for eight materials. These show effects broadly comparable in magnitude to the shell models but more varied in detail. Notably, some models show for the first time a larger rather than smaller Debye–Waller factor for the deforming ion.

Introduction

At least in the past decade, the accurate measurement of Debye–Waller factors has involved concern that not all of the electron distribution of an atom vibrates by the same amount. On the theoretical side one is also concerned that accuracy in calculating the core Debye–Waller factor is wasted if there are moderately

0108-7673/83/040533-06$01.50